Systematic analysis of RNAi-accessible SARS-CoV-2 replication steps identifies ORF1 as promising target

Shubhankar Ambike
Institute of Virology,Technical University / Helmholtz Center Munich https://orcid.org/0000-0003-1089-459X

Cho-Chin Cheng
Institute of Virology,Technical University / Helmholtz Center Munich

Suliman Afridi
Institute of Virology,Technical University / Helmholtz Center Munich

Martin Feuerherd
Institute of Virology,Technical University / Helmholtz Center Munich https://orcid.org/0000-0002-5272-6503

Philipp Hagen
Institute of Virology,Technical University / Helmholtz Center Munich

Vincent Grass
Technical University of Munich https://orcid.org/0000-0001-7710-4789

Olivia Merkel
Department of Pharmacy, Pharmaceutical Technology and Biopharmaceutics, Ludwig- Maximilians-Universität München https://orcid.org/0000-0002-4151-3916

Andreas Pichlmair
Technical University of Munich https://orcid.org/0000-0002-0166-1367

Chunkyu Ko
Institute of Virology, School of Medicine, Technical University of Munich / Helmholtz Zentrum München

Thomas Michler (thomas.michler@tum.de)
Institute of Virology,Technical University / Helmholtz Center Munich https://orcid.org/0000-0002-4174-3316

Article

Keywords: SARS-CoV-2, (si)RNAs, RNAi, COVID-19, ORF1

Posted Date: December 1st, 2020

DOI: https://doi.org/10.21203/rs.3.rs-105129/v2

Abstract

A promising approach to tackle the Severe Acute Respiratory Syndrome Coronavirus-2 (SARS-CoV-2) could be small interfering (si)RNAs. The proof of concept that SARS-CoV-2 can be inhibited with siRNAs, however, is missing. Here, we report that siRNAs can target genomic RNA (gRNA) of SARS-CoV-2 after cell entry, terminating replication before start of transcription and preventing cytopathic effects. Coronaviruses replicate via negative sense intermediate transcripts using a unique discontinuous transcription process. As a result, each viral RNA contains identical sequences at the 5’ and 3’ end. Surprisingly, siRNAs were not active against intermediate negative sense transcripts. Targeting sequences shared by different viral transcripts allowed simultaneous suppression of gRNA and subgenomic (sg)RNAs by a single siRNA. The most effective suppression of viral replication and spread, however, was achieved by siRNAs targeting open reading frame 1 (ORF1) which is solely part of gRNA. We propose two independent mechanisms for this: An increased accessibility of translational-active ORF1 before the start of transcription, as well as highly abundant sgRNAs out-competing siRNAs that target common sequences of transcripts. Our work encourages the development of siRNA-based therapies for COVID-19 and suggests that an early therapy start, together with targeting ORF1, might be key for high antiviral efficacy.

Introduction

Severe Acute Respiratory Syndrome Coronavirus-2 (SARS-CoV-2) is causing a pandemic with so far unforeseeable consequences on global health, politics and economy. SARS-CoV-2, like other coronaviruses affecting humans, is mainly transmitted via respiratory secretions (1) and replicates primarily in respiratory epithelial cells (2). Due to its lytic cell cycle (3), it causes severe endothelial injury and widespread microangiopathy (4), which can result in respiratory failure and death. While some progress has been made by repurposing the RNA polymerase inhibitor Remdesivir (5) or by ameliorating SARS-CoV-2 induced lung injury using Dexamethason (6), lethality of COVID-19 remains high (7). A promising alternative approach could be to deliver small interfering (si)RNAs (8-11) to the respiratory tract by inhalation (12) and induce degradation of viral RNAs by the RNA-interference (RNAi) machinery. Studies performed with Severe Acute Respiratory Syndrome Coronavirus-1 (SARS-CoV-1) or Middle East Respiratory Syndrome Coronavirus (MERS-CoV), showed that siRNAs can silence viral RNA and relieve symptoms caused by related coronaviruses (13-17). However, while several publications have proposed siRNAs as potential therapeutic also for COVID-19 (8-11), until today there is no proof that SARS-CoV-2 can be inhibited by siRNAs, not to mention a detailed systematic analysis, which replication steps are accessible for RNAi.

SARS-CoV-2, as other coronaviruses, has a positive sense, single-stranded RNA genome with a length of approximately 30,000 nucleotides. Following binding to the cellular receptor angiotensin-converting enzyme 2 (18), the virus is taken up via endocytosis (19). After fusion with the endosomal membrane (20), the ribonucleocapsid is released into the cytoplasm. Here, the viral genome serves as template for initial translation of the polyprotein 1ab (pp1b) from Open Reading Frame 1 (ORF1) by the

cellular ribosomal machinery. Pp1ab is cleaved into 16 non-structural proteins (NSPs) of which several assemble around the viral genome to form the replication/transcription complex (RTC) (21). As for other positive sense RNA viruses, transcription does not take place in the cytosol, but exclusively within double-membrane vesicles (22). Therefore, the viral RTC associates with endoplasmic reticulum membranes to form so-called viral replication organelles (ROs). Here, the viral genome serves as template for transcription of full-length progenitor genomic (g)RNA as well as subgenomic (sg)RNAs encoding for structural (S, envelope protein [E], membrane protein [M], Nucleocapsid [N]) as well as accessory proteins (3a, 6, 7a, 7b, 8 and 10) (23). As a results of the discontinuous transcription (24,25), each coronaviral RNA contains an identical 3´ (the ∼70 nucleotides long leader sequence [L]) as well as 5’ end (N ORF and 3´ untranslated region [3´UTR]) (23). Next, sgRNAs are released from ROs (26), translated into the corresponding protein and gRNA packaged by the structural proteins to assemble progeny virions.

Coronaviruses protect their RNA well. Besides the envelope and capsid protecting virions, nucleocapsid proteins bind directly to the viral genome. Thus, even between uncoating and incorporation into double-membraned ROs, the genome is not present as naked RNA (27). Furthermore, while sgRNAs are exported from ROs for translation, this does not seem to be the case for gRNA which remains associated with double-membraned vesicles (26). Currently, it is not clear whether the different viral RNA species produced during replication are accessible for an RNAi-based therapy. Furthermore, certain viral components might be essential for replication, whereas the suppression of others might be tolerated by the virus. Thus, suppression of reporter constructs as often performed during siRNA development does not accurately predict the effect of siRNAs on viral replication and spread. To shed light upon these questions, we systematically analyzed which steps of the SARS-CoV-2 life cycle can be targeted by siRNA and how this would affect viral replication.

Materials And Methods

siRNA design and synthesis

The siRNAs used in the study were designed using siDirect (http://sidirect2.rnai.jp) and siSPOTR (https://sispotr.icts.uiowa.edu/sispotr/index.html) online tools (28-30), structured upon guidelines delineated from previous findings (31-34). We designed siRNAs against four regions of the SARS-CoV-2 genome: Leader sequence, ORF1, Nucleocapsid (N) and 3’ untranslated region (3’UTR), based on the full-length reference sequence available on RefSeq database (NCBI Accession number: NC_045512.2). The siRNAs were designed with an asymmetric design (28) and occasional G:U wobbles (35) for improved specificity (Supplementary Table S1). Two additional siRNAs targeting GFP and Firefly Luciferase were designed as negative controls. The luciferase-specific siRNA served as control for infection experiments and the GFP-specific siRNA for experiments in which Luciferase reporters were used. The siRNAs were purchased in desalted form (Microsynth AG, Balgach, Switzerland), resuspended and maintained in RNAse free water upon arrival. Activity of siRNAs was tested using luciferase reporters (see below) before proceeding to the SARS-CoV-2 infection models.

Cell lines and seeding

HEK293T cells were maintained in glucose-containing Dulbecco's Modified Eagles Medium (DMEM), supplemented with 10% Fetal Bovine Serum (FBS), 2mM L-Glutamine, 50U/ml Penicillin/Streptomycin, 1% Non-essential Amino acids, and 1mM Sodium Pyruvate (Gibco™- Thermo Fisher Scientific GmbH; Dreieich, Germany). VeroE6 cells were maintained in glucose containing DMEM supplemented with 5% FBS. Mycoplasma contaminations were excluded from all cell lines. Cells were kept at 37°C in humidified incubators at 5% CO2. 200,000 HEK293T cells were plated in poly-L-lysin (Sigma-Aldrich Chemie; Taufkirchen, Germany) treated 24-well plates for reporter assays, 700,000, 150,000, or 20,000 VeroE6 cells were plated in 6-well, 24-well, or 96-well plates (Techno Plastic Products; Trasadingen, Switzerland) respectively for experiments including SARS-CoV-2 infection.

Cloning of luciferase reporters

Initial siRNA screenings, testing of siRNA strand-specific activities and the competition assay (shown in Figure 4D) were performed using the dual luciferase expressing psiCHECK™-2 vector (Promega GmbH; Walldorf, Germany) with siRNA target sites cloned into a multiple cloning site present downstream of the Renilla luciferase translational stop codon. For this, the full-length SARS-CoV-2 leader sequence, both negative and positive sense N sequence, as well as the individual siRNA binding sites of siRNAs targeting ORF1 and the 3'UTR were inserted by cloning via XhoI/NotI digestion (FastDigest™, Thermo Fisher Scientific; Dreieich, Germany). The individual siRNA binding sites and the whole Leader sequence were purchased as single-stranded DNA oligonucleotides, designed to form overhangs mimicking digested oligonucleotide fragments after annealing. For this, equal amounts of complementary oligonucleotides were mixed and heated at 95 °C for five minutes followed by gradual cooling for 2h at 30^0C to allow forming of oligonucleotide duplexes. These were directly used in a ligation reaction with the digested psiCHECK-2™ vector. The positive sense N coding sequence was PCR amplified using primers E-N Fw BamHI and E-N Rev EcoRI from cDNA of SARS-CoV-2 infected VeroE6 cells and cloned into the pcDNA1/Amp plasmid vector. In a next step, the N coding sequence was PCR-amplified using primers N CDS Fw XhoI and N CDS Rev NotI and cloned into the luciferase reporter. The full-length negative sense N gene was purchased as desalted, pre-annealed double-stranded DNA oligonucleotide and used directly for the annealing reaction with digested psiCHECK™-2 vector. A list of used oligonucleotides is given in Supplementary Table S2.

Transfection

siRNAs were either transfected 6h before or 3h after SARS-CoV-2 infection using Lipofectamine RNAiMAX (Thermo Fisher Scientific; Dreieich, Germany). A final concentration of 50nM siRNA was used per well. For transfections before SARS-CoV-2 infection, a reverse-transfection protocol was used. Whereas, for transfections after virus infection, a conventional forward-transfection protocol was employed – both according to the manufacturer's instructions. All transfection experiments were performed with at least three biological replicates. For the pre-selection of siRNAs, the determination of strand specific activities

of N-specific siRNAs, and the competition assay, siRNAs were co-transfected together with respective plasmid expressing a luciferase reporter. In brief, 200ng of reporter plasmid and 6pmol of siRNA were mixed with 1µl of transfection reagent (Lipofectamine 2000, Thermo Fisher Scientific; Dreieich, Germany) diluted with Opti-MEM to a final volume of 100µl. siRNA-plasmid containing transfection complexes were added on top of confluent cells, resulting in 10nM final concentration of siRNA per well. For the pre-screening of siRNAs and the determination of strand specific activities of N-specific siRNAs, constructs were transfected into 85-90% confluent HEK293T cells and for the competition assay into confluent VeroE6 cells.

Dual-Luciferase based reporter assay and competition experiment

As a surrogate model to determine siRNA activity, siRNAs were co-transfected into cells with plasmids expressing dual luciferase reporters. After co-transfecting siRNAs and plasmids (for details see paragraph above), cells were lysed after 48h (siRNA prescreening and strand specific activities) with 100µl Passive Lysis Buffer (Promega GmbH; Walldorf, Germany), and luciferase activity from 10µl cell lysate measured using the Dual Luciferase® Reporter Assay System (Promega GmbH; Walldorf, Germany) according to instructions using a Tecan Infinite 200 PRO Microplate reader (Tecan Group Ltd.; Männedorf, Switzerland). Relative activity of *Renilla* luciferase (normalized to Firefly luciferase activity as an internal transfection control) was indicated as silencing efficiency of the siRNA and compared with a control siRNA targeting GFP or Luciferase. For the competition experiment (shown in Fig. 4D-E), siRNAs and the respective luciferase reporter plasmid were co-transfected into VeroE6 cells as described previously, which were 6h later infected with *wildtype* SARS-CoV-2 (MOI 0.1) and 24h later luciferase activity and knockdown efficacy were determined.

SARS-CoV-2 infection

VeroE6 cells were seeded in 24-well format at least 6h before infection to gain approximately 90-95% confluency at time of infection. The SARS-CoV-2 stock was pre-diluted for a multiple of infection (MOI) of 0.1 in 100µl media. At time of infection, old growth media was removed, and the pre-diluted SARS-CoV-2 solution added to cells. After 1h incubation at 37°C, a medium exchange was performed. Different termination time points were performed from 1 to 24h post infection based on the investigated step of the viral replication cycle. The SARS-CoV-2 *wildtype* virus used in this study was isolated from a patient in March 2020 at Institute of Virology, TU Munich. The full-length sequence was uploaded onto GISAID database (https://www.gisaid.org/) under name *hCoV-19/Germany/BAV-PL-virotum-nacq/2020* and accession ID: EPI_ISL_582134.

Real-time monitoring of virus spread using rSARS-CoV-2-GFP and automated fluorescence analysis with the IncuCyte® Live-Cell Analysis

VeroE6 cells in growth media were seeded at least 6h before infection into 96-well plates to gain approximated 90-95% confluency at time of infection. Cell were then infected with a recombinant SARS-CoV-2, expressing Green Fluorescent Protein (GFP) from a sequence integrated at the ORF7 locus (rSARS-

CoV-2-GFP) (36). For this, the rSARS-CoV-2-GFP virus infection solution was pre-diluted for a MOI of 1 in 50µl growth media. After adding 50µl of the infection solution to cells, media was exchanged after 1h and multi-well plates placed into IncuCyte® Live-Cell Analysis machine and phase contrast as well as fluorescence pictures of the whole well acquired every 4h for three days. Total cell number was determined via phase contrast microscopy and infected cell population using the GFP channel using the IncuCyte S3 software (Essen Bioscience; version 2019B Rev2).

Determination of cell viability

The cell viability was determined using the CellTiter-Blue Cell Viability Assay kit (Promega GmbH, Walldorf, Germany) according to manufacturer's instructions. In brief, VeroE6 cells were reversely transfected in 96-well plate with siRNAs 6h before SARS-CoV-2 infection (MOI 1), and cell viability assessed at different time points. For this, CellTiter-Blue reagent was diluted 1:5 with culture medium and applied to cells for 60 min at 37 °C. A distinct color change was observed in the untreated controls in comparison to the empty well controls. Conversion from resazurin to resorufin was analysed with fluorescence filters 550 / 590 nm at a Tecan Infinite F200 (Tecan Group Ltd.; Männedorf, Switzerland).

Nucleic Acid extraction and qPCR

RNA from cultured cells was extracted with the NucleoSpin RNA kit (Macherey-Nagel; Düren, Germany), and cDNA synthesized with the Superscript™ III First-Strand Synthesis System (Thermo Fisher Scientific; Dreieich, Germany) according to manufacturer's instructions. SARS-CoV-2 transcripts were amplified in subsequent qPCR using primers specific to the N region, essentially covering all the viral transcripts or the RNA dependent RNA polymerase (Rdrp) region, as a measure of gRNA. For quantification of viral RNAs, a standard curve was constructed using plasmids with integrated Rdrp or N sequences. Amount of sgRNA was calculated by subtracting the result of PCR reaction using Rdrp primers from the one using N primers (as full-length gRNA is also detected by the N primers). 18S rRNA was used as a reference gene for relative quantification. All quantitative PCRs were performed on a LightCycler® 480 (Roche Holding AG; Basel, Switzerland) using primers and cycling conditions shown in Table 1.

Strand-specific cDNA synthesis

To individually determine negative or positive sense SARS-CoV-2 RNA, we specifically transcribed RNA of a certain polarity to cDNA. For this, first strand synthesis was performed from total RNA extracts using the SuperScript™ IV First-Strand Synthesis System (Thermo Fisher Scientific; Dreieich, Germany) with primers specific either for positive sense mRNA (Oligo$(dT)_{20}$ primers) or negative sense mRNA (Oligo$(dA)_{20}$ primers). To allow transcription of a house keeping gene also in the reaction transcribing negative sense RNA, primers specific for the 18S rRNA gene (18S cDNA1-3; Table 1) were added to the reaction. A final concentration of 50 µM for all primers combined were used for first strand synthesis reaction and viral RNAs quantified by qPCR as described above.

Primers	Sequence (5'-3')
N CDS Fw XhoI	ATCATACTCGAGATGTCTGATAACGGACCCCA
N CDS Rev NotI	ATCATTGCGGCCGCGGCCTGAGTTGAGTCAGCAC
E-N fw BamHI	GGTGGTGGATCCTGAGCCTGAAGAACATGTCC
E-N Rev EcoRI	GGTGGTGAATTCAGCTCTCCCTAGCATTGTTC
Oligo$(dT)_{20}$	TTTTTTTTTTTTTTTTTTTT
Oligo$(dA)_{20}$	AAAAAAAAAAAAAAAAAAAA
18S cDNA 1	CCTTCCGCAGGTTCACCTAC
18S cDNA 2	CCTCCAATGGATCCTCGT
18S cDNA 3	TAATCATGGCCTCAGTTCCG
18S qPCR	Fw: AAACGGCTACCACATCCA Rev: CCTCCAATGGATCCTCGT
N qPCR	Fw: GACCCCAAAATCAGCGAAAT Rev: TCTGGTTACTGCCAGTTGAATCTG
RDRP qPCR	Fw:CGTCTGCGGTATGTGGAAAG Rev: TAAGACGGGCTGCACTTACA
PCR cycling conditions:	Initial Denaturation: 95°C 5 Min (Ramp rate 4.4) 45 Cycles: 95°C - 15 seconds (Ramp rate 4.4) 55°C - 10 seconds (Ramp rate 2.2) 72°C - 25 seconds (Ramp rate 4.4)

Table1. Oligonucleotides and cycling conditions used during polymerase change reaction. A = Adenine; C = Cytosine; G = Guanine; T = Thymine; Rev = reverse; min = minute; s = second; RDRP = RNA-dependent RNA polymerase

Statistical Analysis

Statistical analysis was performed with GraphPad Prism (version 8.4.3) for Mac. Normally distributed samples were analyzed using student T-test for independent samples when comparing two groups and with One-way Anova with Dunnett´s multiple comparison correction when comparing three or more groups. Statistical differences of non-normally distributed data were calculated for two groups using Mann-Whitney U or Kruskal-Wallis with Dunn´s multiple comparison correction tests when comparing three or more groups. p-values <0.05 were considered significant.

Results

Targeting the genome of incoming SARS-CoV-2 terminates replication before start of transcription and prevents cytopathy

Following the events in viral replication cycle, first, we investigated whether siRNAs can directly target the incoming genome of SARS-CoV-2 after cell entry. We chose ORF1 as target region, as it is only contained in full-length genomic, but not sgRNAs (23). We individually transfected three siRNAs which were active in previous luciferase reporter screens (Supplementary Figure S2A) into VeroE6 cells. After 16h, cells were infected with the GFP-expressing rSARS-CoV-2-GFP vector and viral infection and spread monitored by quantifying GFP^+ cells every 4h over the course of three days (Figure 1A, top). As the ORF1-specific siRNAs do not target the transcript from which GFP is expressed, a suppression of GFP expression would indicate that siRNAs targeted full-length gRNA (Figure 1A, bottom). Indeed, we found the number of GFP^+ cells reduced to approximately 50% by each of the tested siRNAs (Figure 1B-D). Importantly, this

difference was already present at the earliest time point (12h post infection [p.i.]) with detectable GFP signal (Figure 1B), indicating that genomes of incoming virus were successfully targeted. We confirmed this by repeating the experiment using *wildtype* SARS-CoV-2 but lysed the cells 24h p.i. and quantified SARS-CoV-2 gRNA by reverse-transcriptase quantitative PCR (RT-qPCR). As indicated by our first experiment, gRNA was reduced in groups pre-treated with the ORF1-specific siRNAs (Figure 1E). To further confirm that indeed genomes of incoming virus were degraded, we transfected cells with a pool of three ORF1-specific siRNAs 6h before infection with *wildtype* SARS-CoV-2 and quantified intracellular viral RNAs at different time points. Viral RNAs were further differentiated into full-length gRNA and sgRNAs (see methods for details). We found that gRNA was reduced as early as 1h p.i. (Figure 1F), before sgRNAs were synthesized (Figure 1G). Treatment with ORF1-specific siRNAs prevented sgRNA expression (Figure 1G), reduced morphologic changes (Figure 1H), and improved metabolic rate of cells (Figure 1I). Taken together, our data proves that siRNAs can target the genome of SARS-CoV-2 and terminate viral replication at an early replication step preventing cytopathy.

Negative sense SARS-CoV-2 RNAs are not accessible for siRNA therapy

Currently it is unclear if both, negative and positive sense coronaviral RNA, or only RNA with a certain polarity is accessible for RNAi silencing. This question is particularly interesting when designing therapeutic siRNAs, as potentially both strands of the siRNA could convey antiviral activity. To gain a more detailed understanding on the kinetic of RNA synthesis during SARS-CoV-2 replication, we lysed *wildtype* SARS-CoV-2-infected VeroE6 cells at different time points. Positive and negative sense viral RNAs were individually quantified by strand specific first strand synthesis (see Methods). Negative sense gRNA was detected in low quantities already 1h p.i., but strongly increased at 6h p.i. when it was more abundant than positive sense gRNA (Figure 2A). In contrast, sgRNAs started to appear only at 6h p.i. (Figure 2B). Consistent with other coronaviruses, lower amounts of negative sense sgRNAs were detected as compared to their positive sense counterparts (37). We now investigated whether negative sense SARS-CoV-2 RNA is accessible for RNAi-mediated silencing. We developed siRNAs that specifically targeted either negative or positive sense SARS-CoV-2 RNA. We chose the N ORF as target region, as it is also part of sgRNAs which are – in contrast to gRNA – exported from ROs (26) and should therefore be easily accessible for siRNAs. siRNA strand-specific activity was validated by co-transfecting siRNAs with reporter plasmids expressing either the positive or negative sense N coding sequence incorporated downstream to *Renilla* luciferase gene (see scheme in Figure 2C and methods). The majority of siRNAs showed high selectivity against the RNA strand they were designed (Supplementary Figure S1). We chose siRNAs with almost exclusive activity against either the positive or negative sense reporter (Figure 2D). To our surprise, only siRNAs active against positive sense N ORF succeeded in reducing sgRNA of *wildtype* SARS-CoV-2 (Figure 2E), thereby inhibiting viral spread in the rSARS-CoV-2-GFP model (Figure 2F). In summary, our data proves that negative sense SARS-CoV-2 RNAs are inaccessible for RNAi.

Targeting common regions of SARS-CoV-2 transcripts allows simultaneous suppression of gRNA and sgRNAs, but leads to loss of efficacy

We further went on to investigate whether targeting the common regions shared by all SARS-CoV-2 transcripts (L, N ORF and 3´UTR; Figure 3A) would allow simultaneous suppression of gRNA as well as sgRNAs. In contrast to inceptive experimental setup, we infected VeroE6 cells with *wildtype* SARS-CoV-2 and afterwards transfected siRNAs targeting either the common regions of transcripts (shown in red) or ORF1 (blue) which is contained only in gRNA. For each target region, we used a pool of three siRNAs which previously showed similar activities against luciferase reporters (Supplementary Figure S2A). As expected, ORF1-specific siRNAs suppressed only gRNA, whereas siRNAs targeting common regions of transcripts suppressed gRNA and sgRNAs (Figure 3B). We next investigated how targeting sgRNAs in addition to gRNA would affect antiviral efficacy. Therefore, we infected VeroE6 cells with rSARS-CoV-2-GFP and 3h later, individually transfected three siRNAs for each target region. Viral spread was evaluated by quantifying GFP^+ cells every 4h over a course of three days. All tested siRNAs reduced GFP^+ cells compared to the control groups. siRNAs targeting gRNA and sgRNAs strongly suppressed GFP expression until 40h p.i. (as they also targeted the GFP-transcript; Supplementary Figure 2B, C) but then, the number of GFP^+ cells increased exponentially (Figure 3C and Supplementary Figure 2D, E). In contrast, groups treated with ORF1-specific siRNAs inhibited viral spread more efficiently, showing a linear and generally slower increase of GFP^+ cells (Figure 3C). In summary, our data indeed showed a concurrent suppression of genomic and subgenomic viral RNAs by siRNAs targeting the common regions in the viral transcripts. On the other hand, the ORF1 specific siRNAs which solely target SARS-CoV-2 gRNA, subdue viral replication more efficiently as compared to siRNAs that additionally targeted sgRNAs.

Targeting ORF1 with siRNAs prevents RNA transcription and out-competition by sgRNAs

To investigate which replication step was more efficiently targeted by ORF1-specific siRNAs, we compared transfection of siRNAs before and after infection with *wildtype* SARS-CoV-2 and assessed viral RNA knockdown after 24h. While ORF1-specific siRNAs showed a trend towards slightly stronger efficacy compared to siRNAs targeting common regions when transfected after infection, the difference was significantly enhanced when siRNAs were transfected before infection (Supplementary Figure S3). This indicated that ORF1-specific siRNAs had an advantage while targeting an early replication step of SARS-CoV-2. To further pinpoint which replication step was primarily affected, we transfected VeroE6 cells 6h before infection with *wildtype* SARS-CoV-2 and analyzed the effect on viral RNAs at different time points. Indeed, ORF1-specific siRNAs showed an enhanced knockdown of gRNA already 1h p.i. (Figure 4A) leading to decreased transcription of negative sense gRNA (Figure 4B) and sgRNAs (Figure 4C). Taken together, our data demonstrates that ORF1-specific siRNAs more efficiently targeted SARS-CoV-2 gRNA, ergo, more efficiently prevented transcription, than siRNAs targeting common regions of transcripts.

We hypothesized, that a second reason for the decreased efficacy of siRNAs targeting gRNA as well as sgRNA could be the high abundance of sgRNAs outcompeted siRNAs and/or RNA-induced Silencing Complexes (RISC). To test this hypothesis, we co-transfected siRNAs targeting the different SARS-CoV-2 regions together with their respective luciferase reporter. After 6h, we infected cells with *wildtype* SARS-CoV-2 and analyzed how SARS-CoV-2 replication in cells would affect silencing of the luciferase reporter (Figure 4D). Of note, in this experimental setting, both SARS-CoV-2 RNAs and mRNA transcribed from a

luciferase reporter plasmid can be targeted by the respective siRNAs. Indeed, we found that silencing of luciferase reporters by siRNAs which targeted gRNA and sgRNAs was significantly impaired by SARS-CoV-2 replication. This was not observed for the ORF1-specific siRNA which suppressed the luciferase reporter with same efficacy in both, infected as well as non-infected cells (Figure 4E). In summary, our data show that two mechanisms, a more efficient targeting of viral genomes by ORF1-specific siRNAs, as well as an impaired RNAi silencing affecting siRNAs targeting additionally sgRNAs, are responsible for the observed differences of siRNA activities.

Discussion

A promising approach to develop antiviral therapies against SARS-CoV-2 constitute siRNAs, which is pursued by several academic and industry groups (38,39). We provide the first proof that SARS-CoV-2 replication and spread can be efficiently controlled using siRNAs. We found that siRNAs, when given in a prophylactic setting, can target the genome of SARS-CoV-2 after cell entry and terminate replication before start of transcription. To our surprise, targeting solely gRNA resulted in a stronger antiviral efficacy than a simultaneous targeting of gRNA and sgRNA. We show that two independent mechanisms were responsible for this. First, ORF1-specific siRNAs more efficiently targeted genomes of SARS-CoV-2 before start of transcription. As ORF1 is the only translational active region before formation of RTC and ROs, the other genomic regions were probably less accessible for the RNAi machinery, due to secondary RNA structures (40) or as they are shielded by nucleocapsid proteins (41). Second, the impaired RNAi silencing affecting siRNAs targeting gRNA and sgRNAs could result from the high abundance of sgRNAs outcompeting siRNAs and/or RISC complexes. This notion appears especially plausible as Kim et al. showed that roughly 2/3rd of the transcriptome of infected cells are made up of SARS-CoV-2 RNAs of which almost all contain the targeted sequences (23). Our findings on a first look might contradict a previous report which described that targeting the leader sequence of SARS-CoV-1 with siRNAs would be more efficacious than targeting the S ORF (13). Several factors could explain differences found in our study. First of all, SARS-CoV-1, which – while being the closest related virus – has an amino acid sequence homology of only between 40-94% depending on the ORF (42), thus findings might not be applicable to SARS-CoV-2. Also, Li et al. compared an siRNA targeting the Leader sequence to siRNAs targeting the S gene, but not to ORF1-specific siRNAs. As we speculate that one possible mechanism for the enhanced efficacy of ORF1 siRNA stems from ORF1 being the only translational active region before start of transcription, our finding might not apply to siRNAs targeting the S ORF. Third, Li et al. compared only a single Leader-specific siRNA to two S-specific siRNAs questioning if the finding can be generalized to the target region or if intra-individual differences of siRNA activity were responsible for the observed differences. Regarding the reason why negative sense SARS-CoV-2 RNA was not accessible for siRNA-silencing, the most plausible explanation to us is that negative sense RNA – in contrast to positive sense RNAs – are not exported from ROs. As probably no RISC complexes are present within the ROs, activity of siRNA is restricted to RNAs which have either not yet entered ROs (gRNA of incoming virus) or positive sense sgRNAs which are exported from ROs for translation. This is in line with the notion that negative sense RNAs are not translated to proteins, creating no necessity to export them into cytosol.

Several factors that have to be considered for clinical application were not addressed in our study. During siRNA design, we did not take the conservation of target regions into account which could affect occurrence of resistance mutations under therapy. However, as ORF1 shows a relatively high conservation compared to other regions of the SARS-CoV-2 genome (43), it appears plausible that an ORF1-specific siRNA drug candidate with a high resistance barrier could be developed. Also, we did neither chemically modify our siRNAs – which might further enhance activity, stability and tolerability of siRNAs – nor did we use advanced delivery methods which would enhance efficacy an allow clinical application (44-47). These questions should be addressed in further studies to allow development of potent siRNA-based therapies. Especially the identification of the optimal carrier and administration route is an important factor. While pulmonary delivery can be achieved by intranasal (i.n.) or inhalation administration, i.n. administration was chosen as the delivery route in Alnylam's early attempts of delivering siRNA against RSV (48). The big advantage of i.n. delivery is the possibility of administering a liquid formulation as nose drops without the need of nebulizing the formulation. This is particularly of impact for liposomal formulations as they do not withstand shear forces and temperature-related stress during nebulization (49). The biggest disadvantage of i.n. administration, however, is the low pulmonary bioavailability of the administered dose, while a large proportion is swallowed and degraded (50). Inhalation delivery, in contrast, requires aerosol development of a mist or dry powder. For nebulization of macromolecules such as siRNA, vibrating mesh nebulizers are preferred for decreased effects on biomolecule stability (45). Dry powder inhalation offers the advantages of long shelf-lives and enhanced stability of nucleic acid formulations against chemical, physical and microbial factors (46) but faces engineering challenges when nucleic acids nanoformulations need to be transferred into dry powders (51). Such nanoformulations are, however, particularly important for pulmonary delivery where free nucleic acids do not efficiently diffuse through the mucus barrier for subsequent uptake into the epithelium (52). Numerous siRNA nanoformulations exist based on polymers, lipids, peptides and inorganic materials (53), each of which can be improved in efficiency and specificity with different surface modifications such as targeting ligands or membrane-active substances (47).

To our knowledge, there is so far no equally detailed analysis of RNAi-targetable replication steps and RNA species for any positive sense RNA virus. Thus, our results might also be of relevance beyond SARS-CoV-2. The reduction of cytopathic effects achieved by antiviral siRNAs could play out crucial, as endothelial injury has been proposed to trigger pathology in lethal COVID-19 cases (4). Along this line, early therapy starts, or possibly even prophylactic application of siRNAs appears as major benefit. Especially in this setting, targeting ORF1 was advantageous over targeting sequences contained also in sgRNAs which could be a valuable information for designing siRNAs and treatment regimens in clinical studies. Taken together, our study confirms that siRNA-based strategies could allow to develop potent antivirals to reduce pathology of COVID-19, encouraging academia and industry to proceed with ongoing efforts.

DATA AVAILABILITY

All data supporting the findings of this study are available within the article and the supplementary information files.

GISAID database is available at: https://www.gisaid.org/

The siSPOTR and siDirect 2.0 siRNA designing tools are available at: https://sispotr.icts.uiowa.edu/ and http://sidirect2.rnai.jp/

ACCESSION NUMBERS

SARS-CoV-2 reference sequence referred for siRNA designing is available at NCBI RefSeq database with accession number: NC_045512.2

The sequence of SARS-CoV-2 used for infection experiments is available on GISAID database under accession ID: EPI_ISL_582134.

Declarations

ACKNOWLEDGEMENT

We thank Prof. Dr. Volker Thiel for providing the recombinant, GFP-expressing SARS-CoV-2 virus, Theresa Asen for help with cell culture and Prof. Dr. Ulrike Protzer for general support such as providing the *wildtype* SARS-CoV-2 virus.

FUNDING

This study was supported by a research grant of the Bavarian State Government by the *Förderprogramm Corona-Forschung* and the Else Kroener-Research College `Microbial triggers as cause of disease´ to T.M. and ERC consolidator grant (ERC-CoG ProDAP, 817798), the German Research Foundation (PI1084/5, TRR178/TP11 TRR 237/A07) and the German Federal Ministry of Education and Research (COVINET) to A.P.

CONFLICT OF INTEREST

T.M. is an ad Hoc advisor for VIR Biotechnology and received research grants by Alnylam Pharmaceuticals and Gilead Sciences. M.F. is a consultant for Dr. Hönle AG.

References

1. Wölfel, R., Corman, V.M., Guggemos, W., Seilmaier, M., Zange, S., Müller, M.A., Niemeyer, D., Jones, T.C., Vollmar, P., Rothe, C. *et al.* (2020) Virological assessment of hospitalized patients with COVID-2019. *Nature*, **581**, 465-469.
2. Sungnak, W., Huang, N., Bécavin, C., Berg, M., Queen, R., Litvinukova, M., Talavera-López, C., Maatz, H., Reichart, D., Sampaziotis, F. *et al.* (2020) SARS-CoV-2 entry factors are highly expressed in nasal

epithelial cells together with innate immune genes. *Nat Med*, **26**, 681-687.

3. Chu, H., Chan, J.F.W., Yuen, T.T.T., Shuai, H., Yuan, S., Wang, Y., Hu, B., Yip, C.C.Y., Tsang, J.O.L., Huang, X. *et al.* (2020), *Lancet Microbe*, Vol. 1, pp. e14-23.
4. Ackermann, M., Verleden, S.E., Kuehnel, M., Haverich, A., Welte, T., Laenger, F., Vanstapel, A., Werlein, C., Stark, H., Tzankov, A. *et al.* (2020) Pulmonary Vascular Endothelialitis, Thrombosis, and Angiogenesis in Covid-19. *N Engl J Med*, **383**, 120-128.
5. Beigel, J.H., Tomashek, K.M., Dodd, L.E., Mehta, A.K., Zingman, B.S., Kalil, A.C., Hohmann, E., Chu, H.Y., Luetkemeyer, A., Kline, S. *et al.* (2020) Remdesivir for the Treatment of Covid-19 - Final Report. *N Engl J Med*.
6. Horby, P., Lim, W.S., Emberson, J., Mafham, M., Bell, J., Linsell, L., Staplin, N., Brightling, C., Ustianowski, A., Elmahi, E. *et al.* (2020) Effect of Dexamethasone in Hospitalized Patients with COVID-19: Preliminary Report.
7. WHO_Solidarity_trial_consortium, Pan, H., Peto, R., Karim, Q.A., Alejandria, M., Restrepo, A.M.H., Garcia, C.H., Kieny, M.P., Malekzadeh, R., Murthy, S. *et al.* (2020) Repurposed antiviral drugs for COVID-19; interim WHO SOLIDARITY trial results.
8. Kruse, R.L. (2020) Therapeutic strategies in an outbreak scenario to treat the novel coronavirus originating in Wuhan, China. *F1000Res*, **9**, 72.
9. Ghosh, S., Firdous, S.M. and Nath, A. (2020) siRNA could be a potential therapy for COVID-19. *EXCLI J*, **19**, 528-531.
10. Baldassarre, A., Paolini, A., Bruno, S.P., Felli, C., Tozzi, A.E. and Masotti, A. (2020) Potential use of noncoding RNAs and innovative therapeutic strategies to target the 5'UTR of SARS-CoV-2. *Epigenomics*, **12**, 1349-1361.
11. Chowdhury, U.F., Shohan, M. U. S., Hoque, K. I., Beg, M. A., Siam, M. K. S. and Moni, M. A. (2020) Computational Approach to Design Potential siRNA Molecules as a Prospective Tool for Silencing Nucleocapsid Phosphoprotein and Surface Glycoprotein Gene of SARS-CoV-2. *bioRxiv*, **pp. 2020.04.10.036335.**
12. Chow, M.Y.T., Qiu, Y. and Lam, J.K.W. (2020) Inhaled RNA Therapy: From Promise to Reality. *Trends in pharmacological sciences*, **41**.
13. Li, T., Zhang, Y., Fu, L., Yu, C., Li, X., Li, Y., Zhang, X., Rong, Z., Wang, Y., Ning, H. *et al.* (2005) siRNA targeting the leader sequence of SARS-CoV inhibits virus replication. *Gene Ther*, **12**, 751-761.
14. Shi, Y., Yang, D.H., Xiong, J., Jia, J., Huang, B. and Jin, Y.X. (2005) Inhibition of genes expression of SARS coronavirus by synthetic small interfering RNAs. *Cell Res*, **15**, 193-200.
15. Nur, S.M., Hasan, M.A., Amin, M.A., Hossain, M. and Sharmin, T. (2015) Design of Potential RNAi (miRNA and siRNA) Molecules for Middle East Respiratory Syndrome Coronavirus (MERS-CoV) Gene Silencing by Computational Method. *Interdiscip Sci*, **7**, 257-265.
16. Li, B.J., Tang, Q., Cheng, D., Qin, C., Xie, F.Y., Wei, Q., Xu, J., Liu, Y., Zheng, B.J., Woodle, M.C. *et al.* (2005) Using siRNA in prophylactic and therapeutic regimens against SARS coronavirus in Rhesus macaque. *Nat Med*, **11**, 944-951.

17. Tang, Q., Li, B., Woodle, M. and Lu, P.Y. (2008) Application of siRNA against SARS in the rhesus macaque model. *Methods Mol Biol*, **442**, 139-158.
18. Hoffmann, M., Kleine-Weber, H., Schroeder, S., Krüger, N., Herrler, T., Erichsen, S., Schiergens, T.S., Herrler, G., Wu, N.H., Nitsche, A. *et al.* (2020) SARS-CoV-2 Cell Entry Depends on ACE2 and TMPRSS2 and Is Blocked by a Clinically Proven Protease Inhibitor. *Cell*, **181**, 271-280.e278.
19. Burkard, C., Verheije, M.H., Wicht, O., van Kasteren, S.I., van Kuppeveld, F.J., Haagmans, B.L., Pelkmans, L., Rottier, P.J., Bosch, B.J. and de Haan, C.A. (2014) Coronavirus cell entry occurs through the endo-/lysosomal pathway in a proteolysis-dependent manner. *PLoS Pathog*, **10**, e1004502.
20. Shang, J., Wan, Y., Luo, C., Ye, G., Geng, Q., Auerbach, A. and Li, F. (2020) Cell entry mechanisms of SARS-CoV-2. *Proc Natl Acad Sci U S A*, **117**, 11727-11734.
21. Fehr, A.R. and Perlman, S. (2015) Coronaviruses: an overview of their replication and pathogenesis. *Methods Mol Biol*, **1282**, 1-23.
22. Snijder, E.J., Limpens, R.W.A.L., de Wilde, A.H., de Jong, A.W.M., Zevenhoven-Dobbe, J.C., Maier, H.J., Faas, F.F.G.A., Koster, A.J. and Bárcena, M. (2020) A unifying structural and functional model of the coronavirus replication organelle: Tracking down RNA synthesis. *PLoS Biol*, **18**, e3000715.
23. Kim, D., Lee, J.Y., Yang, J.S., Kim, J.W., Kim, V.N. and Chang, H. (2020) The Architecture of SARS-CoV-2 Transcriptome. *Cell*, **181**, 914-921 e910.
24. Sola, I., Almazan, F., Zuniga, S. and Enjuanes, L. (2015) Continuous and Discontinuous RNA Synthesis in Coronaviruses. *Annu Rev Virol*, **2**, 265-288.
25. Enjuanes, L., Almazan, F., Sola, I. and Zuniga, S. (2006) Biochemical aspects of coronavirus replication and virus-host interaction. *Annu Rev Microbiol*, **60**, 211-230.
26. van Hemert, M.J., van den Worm, S.H., Knoops, K., Mommaas, A.M., Gorbalenya, A.E. and Snijder, E.J. (2008) SARS-coronavirus replication/transcription complexes are membrane-protected and need a host factor for activity in vitro. *PLoS Pathog*, **4**, e1000054.
27. Chang, C.K., Hou, M.H., Chang, C.F., Hsiao, C.D. and Huang, T.H. (2014) The SARS coronavirus nucleocapsid protein–forms and functions. *Antiviral Res*, **103**, 39-50.
28. Boudreau, R.L., Spengler, R.M., Hylock, R.H., Kusenda, B.J., Davis, H.A., Eichmann, D.A. and Davidson, B.L. (2013) siSPOTR: a tool for designing highly specific and potent siRNAs for human and mouse. *Nucleic Acids Res*, **41**, e9.
29. Naito, Y., Yamada, T., Ui-Tei, K., Morishita, S. and Saigo, K. (2004) siDirect: highly effective, target-specific siRNA design software for mammalian RNA interference. *Nucleic Acids Res*, **32**, W124-129.
30. Naito, Y., Yoshimura, J., Morishita, S. and Ui-Tei, K. (2009) siDirect 2.0: updated software for designing functional siRNA with reduced seed-dependent off-target effect. *BMC Bioinformatics*, **10**, 392.
31. Boudreau, R.L., Spengler, R.M. and Davidson, B.L. (2011) Rational design of therapeutic siRNAs: minimizing off-targeting potential to improve the safety of RNAi therapy for Huntington's disease. *Mol Ther*, **19**, 2169-2177.

32. Reynolds, A., Leake, D., Boese, Q., Scaringe, S., Marshall, W.S. and Khvorova, A. (2004) Rational siRNA design for RNA interference. *Nat Biotechnol*, **22**, 326-330.
33. Ui-Tei, K., Naito, Y., Nishi, K., Juni, A. and Saigo, K. (2008) Thermodynamic stability and Watson-Crick base pairing in the seed duplex are major determinants of the efficiency of the siRNA-based off-target effect. *Nucleic Acids Res*, **36**, 7100-7109.
34. Ui-Tei, K., Naito, Y., Takahashi, F., Haraguchi, T., Ohki-Hamazaki, H., Juni, A., Ueda, R. and Saigo, K. (2004) Guidelines for the selection of highly effective siRNA sequences for mammalian and chick RNA interference. *Nucleic Acids Res*, **32**, 936-948.
35. Holen, T., Moe, S.E., Sørbø, J.G., Meza, T.J., Ottersen, O.P. and Klungland, A. (2005) Tolerated wobble mutations in siRNAs decrease specificity, but can enhance activity in vivo. *Nucleic Acids Res*, **33**, 4704-4710.
36. Thi Nhu Thao, T., Labroussaa, F., Ebert, N., V'Kovski, P., Stalder, H., Portmann, J., Kelly, J., Steiner, S., Holwerda, M., Kratzel, A. *et al.* (2020) Rapid reconstruction of SARS-CoV-2 using a synthetic genomics platform. *Nature*, **582**, 561-565.
37. Hagemeijer, M.C., Vonk, A.M., Monastyrska, I., Rottier, P.J. and de Haan, C.A. (2012) Visualizing coronavirus RNA synthesis in time by using click chemistry. *J Virol*, **86**, 5808-5816.
38. Vir Biotechnology, I.a.A.P., Inc. (2020). BUSINESS WIRE, SAN FRANCISCO & CAMBRIDGE, Mass.
39. NEWSWIRE, P. (2020). PR NEWSWIRE, https://www.prnewswire.com/news-releases/sirnaomics-advances-rnai-based-prophylactics-and-therapeutics-to-battle-sari-caused-by-2019-ncov-300993007.html.
40. Rangan, R., Zheludev, I.N. and Das, R. (2020) RNA genome conservation and secondary structure in SARS-CoV-2 and SARS-related viruses. *bioRxiv*.
41. Baric, R.S., Nelson, G.W., Fleming, J.O., Deans, R.J., Keck, J.G., Casteel, N. and Stohlman, S.A. (1988) Interactions between coronavirus nucleocapsid protein and viral RNAs: implications for viral transcription. *J Virol*, **62**, 4280-4287.
42. Grifoni, A., Sidney, J., Zhang, Y., Scheuermann, R.H., Peters, B. and Sette, A. (2020) A Sequence Homology and Bioinformatic Approach Can Predict Candidate Targets for Immune Responses to SARS-CoV-2. *Cell Host Microbe*, **27**, 671-680.e672.
43. Abbott, T.R., Dhamdhere, G., Liu, Y., Lin, X., Goudy, L., Zeng, L., Chemparathy, A., Chmura, S., Heaton, N.S., Debs, R. *et al.* (2020) Development of CRISPR as an Antiviral Strategy to Combat SARS-CoV-2 and Influenza. *Cell*, **181**, 865-876.e812.
44. Weber, S., Zimmer, A. and Pardeike, J. (2014) Solid Lipid Nanoparticles (SLN) and Nanostructured Lipid Carriers (NLC) for pulmonary application: a review of the state of the art. *Eur J Pharm Biopharm*, **86**, 7-22.
45. de Kruijf, W. and Ehrhardt, C. (2017) Inhalation delivery of complex drugs-the next steps. *Curr Opin Pharmacol*, **36**, 52-57.
46. Feldmann, D.P. and Merkel, O.M. (2015) The advantages of pulmonary delivery of therapeutic siRNA. *Ther Deliv*, **6**, 407-409.

47. Kandil, R. and Merkel, M. (2016) Therapeutic delivery of RNA effectors: diseases affecting the respiratory system. *Pharmazie*, **71**, 21-26.
48. DeVincenzo, J., Lambkin-Williams, R., Wilkinson, T., Cehelsky, J., Nochur, S., Walsh, E., Meyers, R., Gollob, J. and Vaishnaw, A. (2010) A randomized, double-blind, placebo-controlled study of an RNAi-based therapy directed against respiratory syncytial virus. *Proc Natl Acad Sci U S A*, **107**, 8800-8805.
49. Weber, S., Zimmer, A. and Pardeike, J. (2014) Solid Lipid Nanoparticles (SLN) and Nanostructured Lipid Carriers (NLC) for pulmonary application: a review of the state of the art. *European Journal of Pharmaceutics and Biopharmaceutics*, **86**, 7-22.
50. Merkel, O.M. and Kissel, T. (2012) Nonviral Pulmonary Delivery of siRNA. *Accounts of Chemical Research*, **45**, 961-970.
51. Keil, T.W.M., Feldmann, D.P., Costabile, G., Zhong, Q., da Rocha, S. and Merkel, O.M. (2019) Characterization of spray dried powders with nucleic acid-containing PEI nanoparticles. *Eur J Pharm Biopharm*, **143**, 61-69.
52. Sanders, N., Rudolph, C., Braeckmans, K., De Smedt, S.C. and Demeester, J. (2009) Extracellular barriers in respiratory gene therapy. *Adv Drug Deliv Rev*, **61**, 115-127.
53. Merkel, O.M., Rubinstein, I. and Kissel, T. (2014) siRNA Delivery to the lung: What's new? *Advanced Drug Delivery Reviews*, **75**, 112-128.

Figures

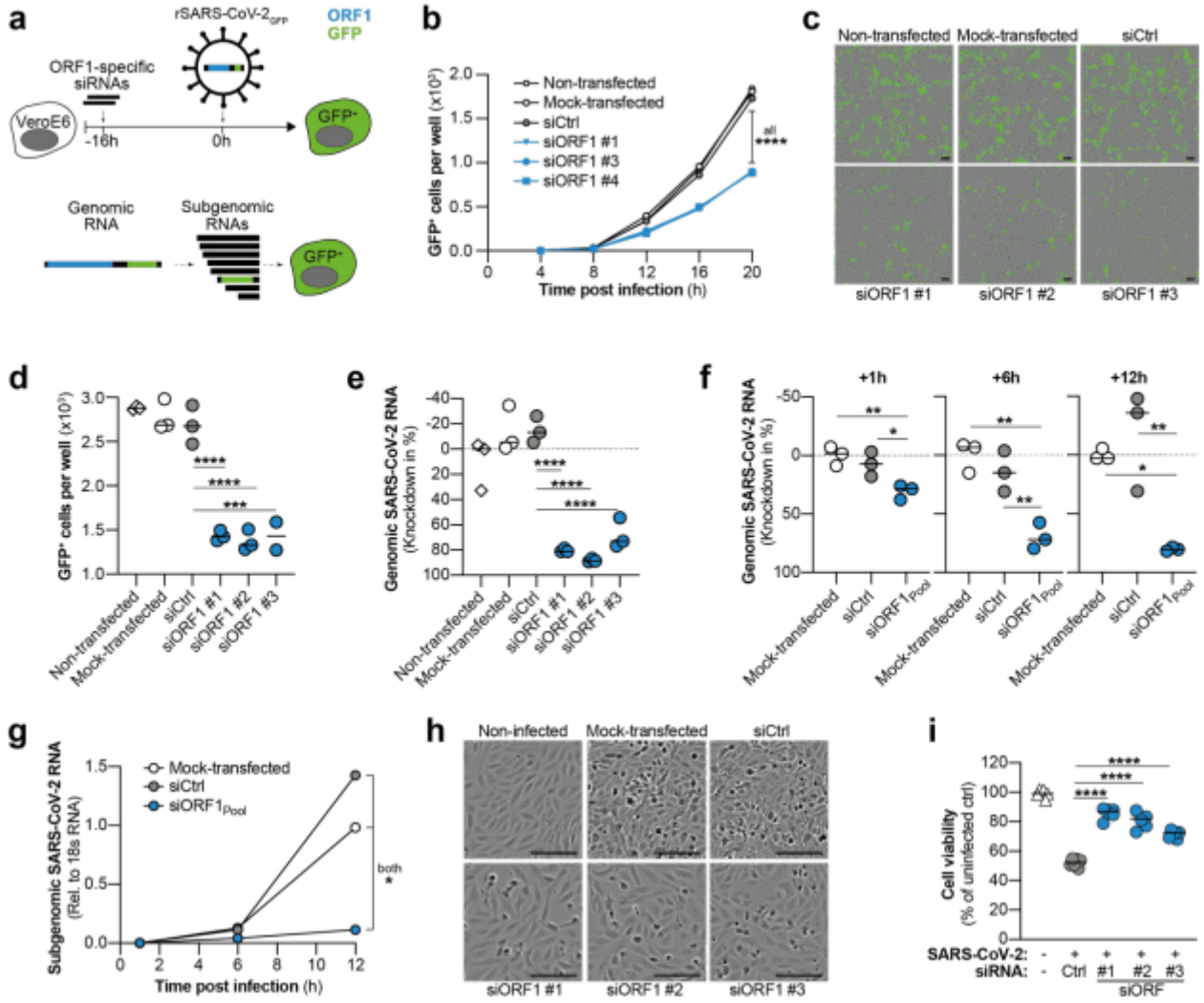

Figure 1

[Please see the manuscript file to view figure caption.]

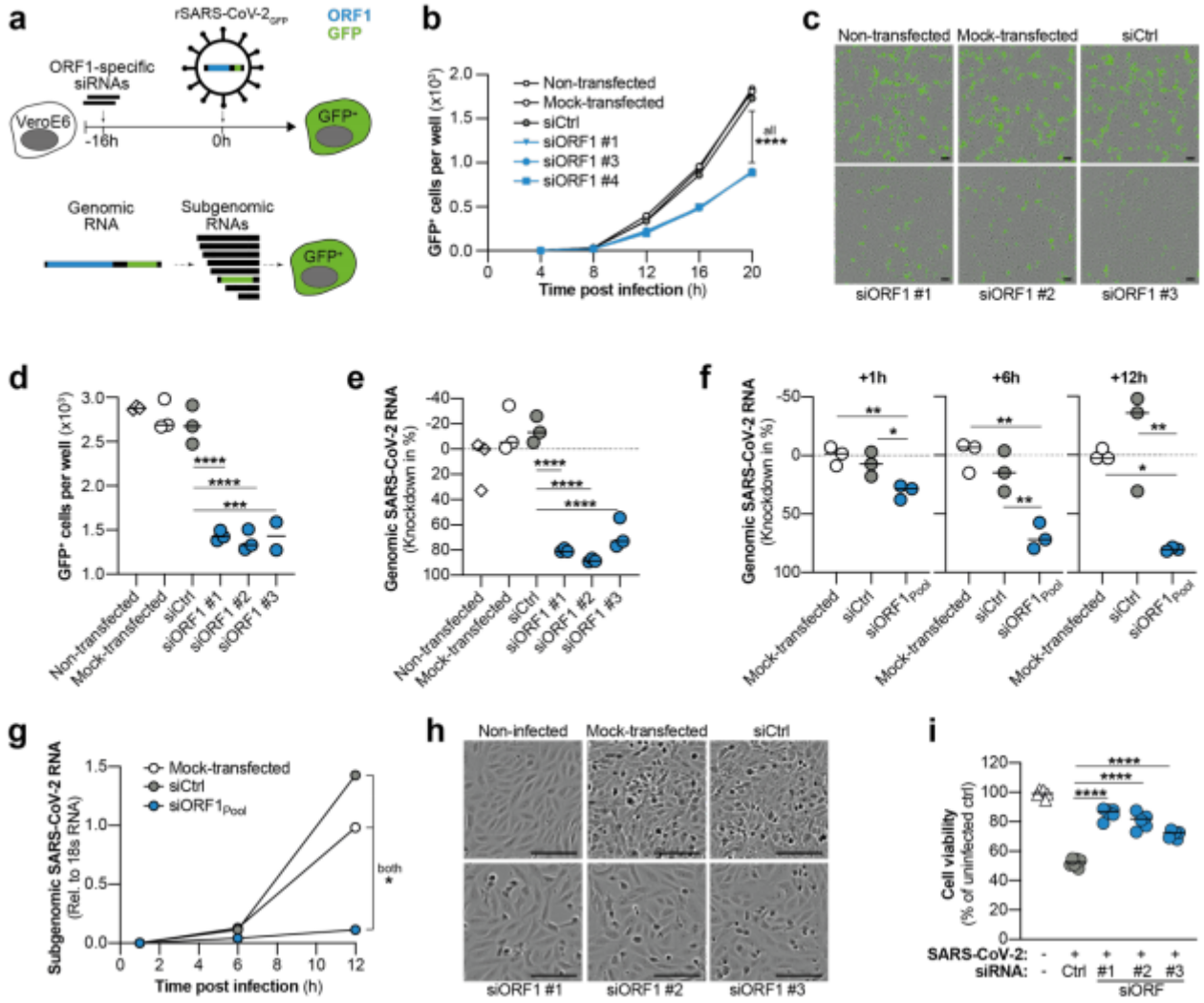

Figure 1

[Please see the manuscript file to view figure caption.]

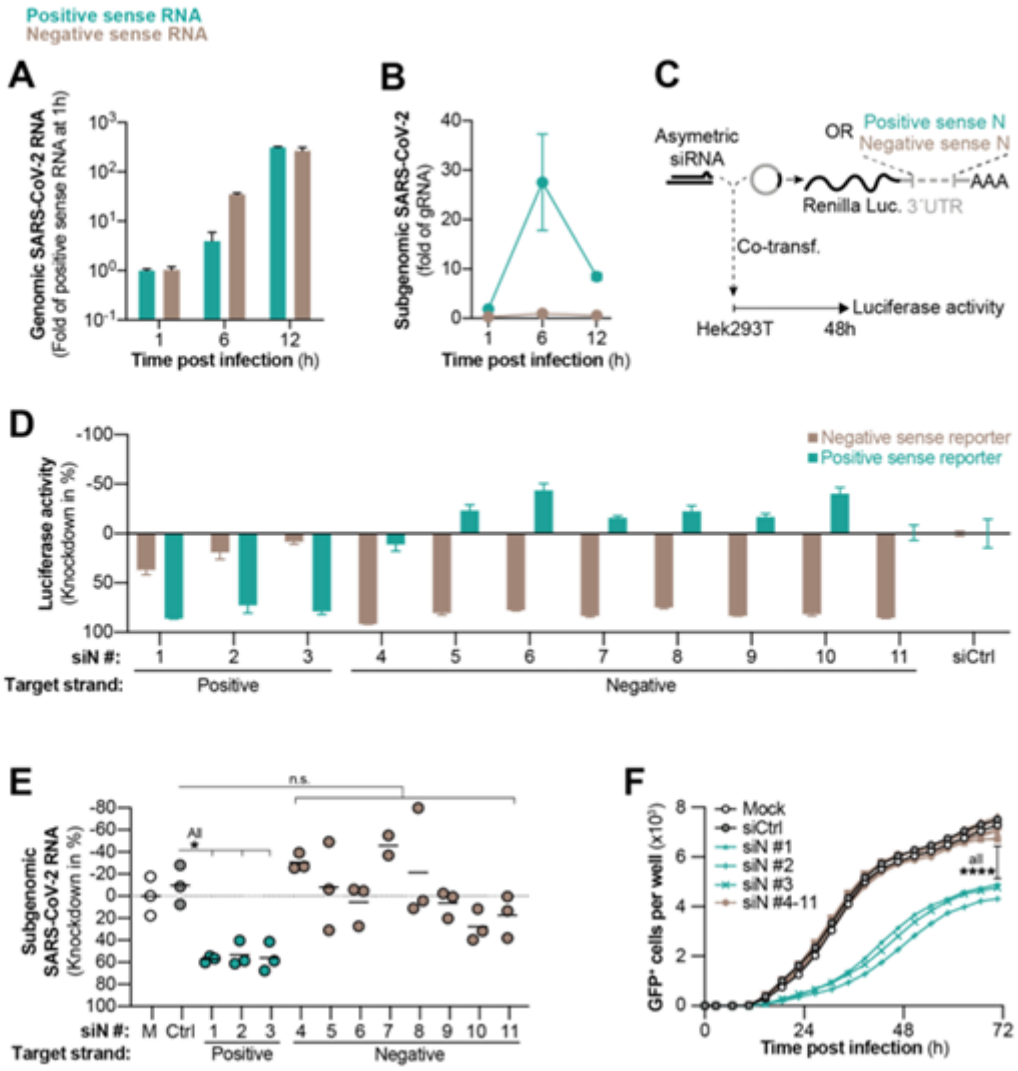

Figure 2

[Please see the manuscript file to view figure caption.]

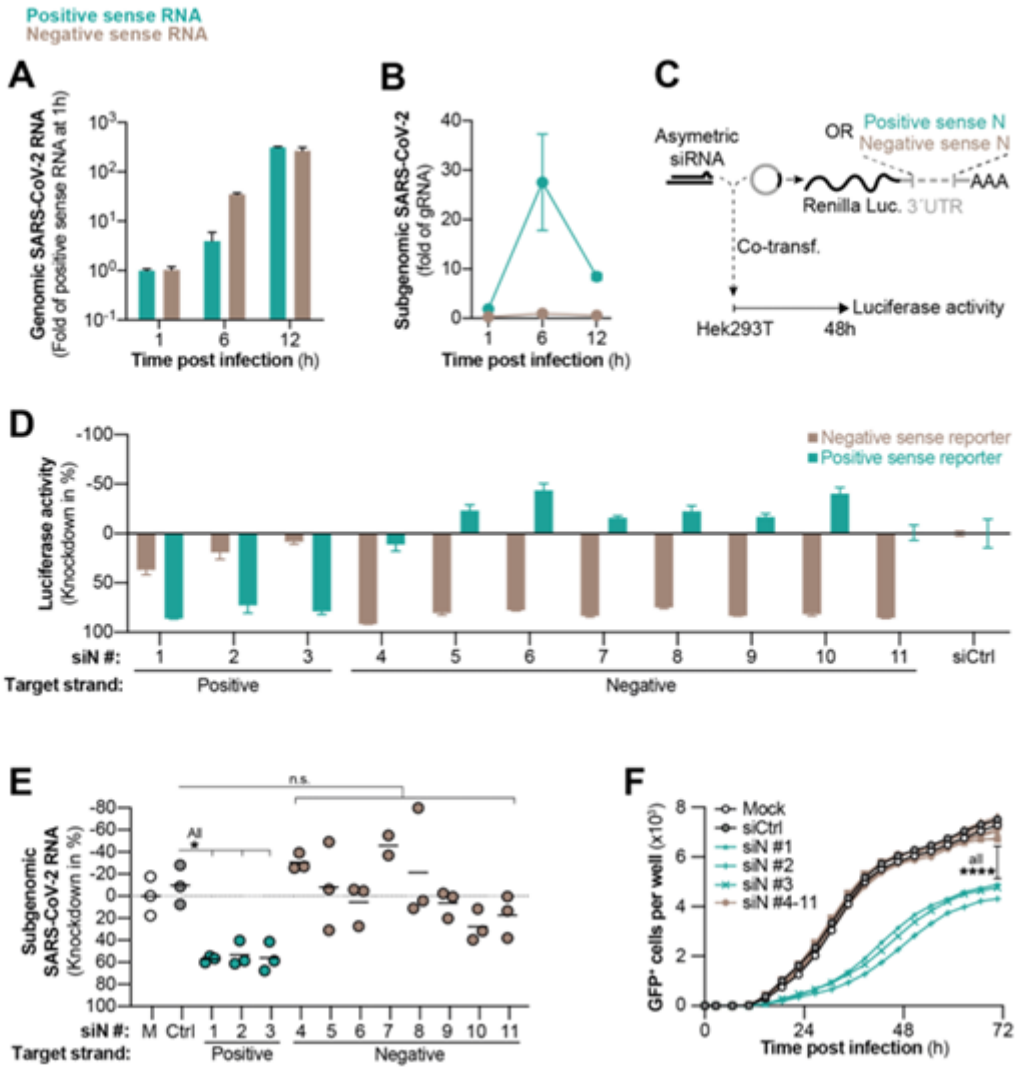

Figure 2

[Please see the manuscript file to view figure caption.]

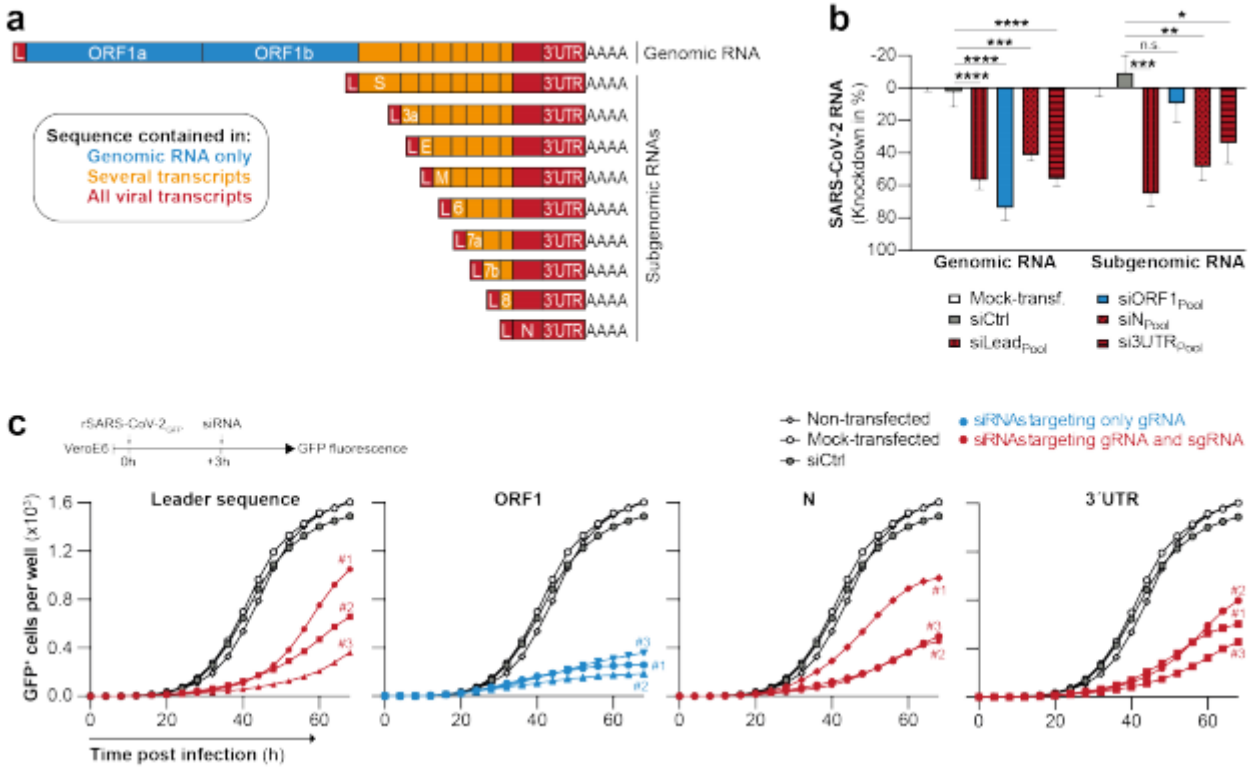

Figure 3

[Please see the manuscript file to view figure caption.]

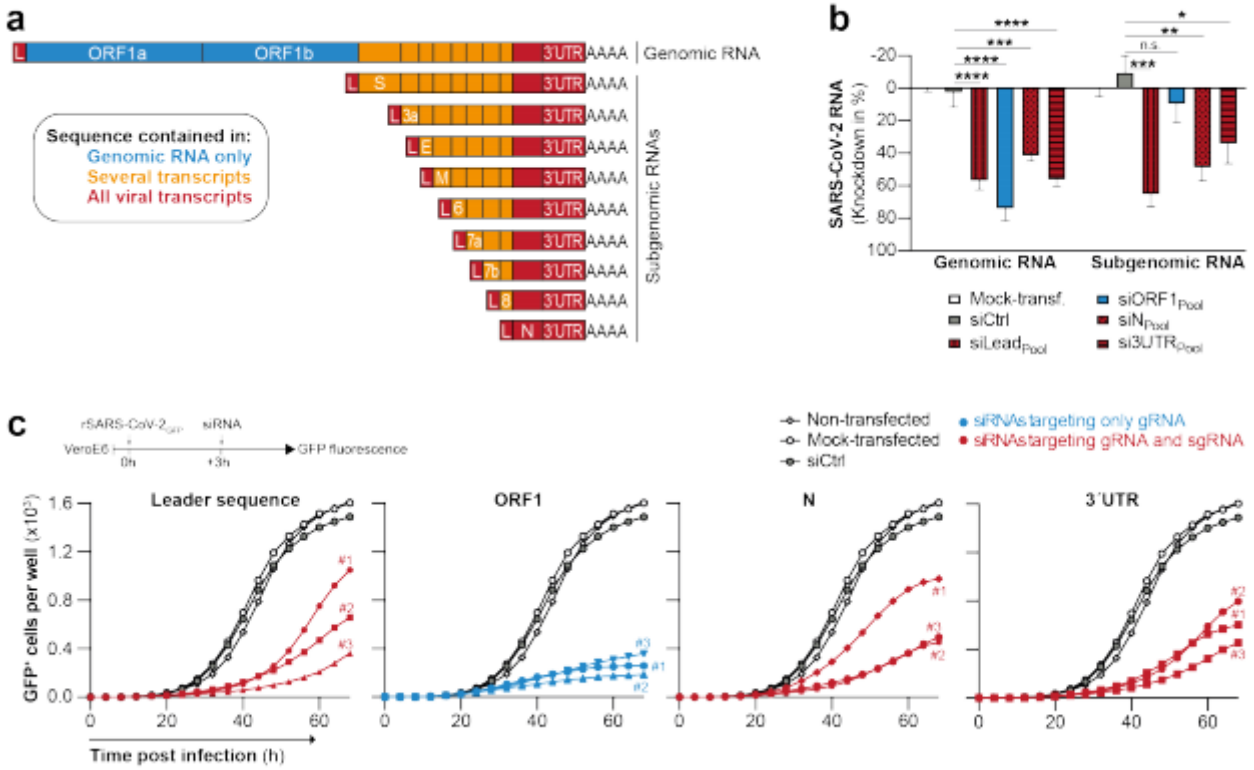

Figure 3

[Please see the manuscript file to view figure caption.]

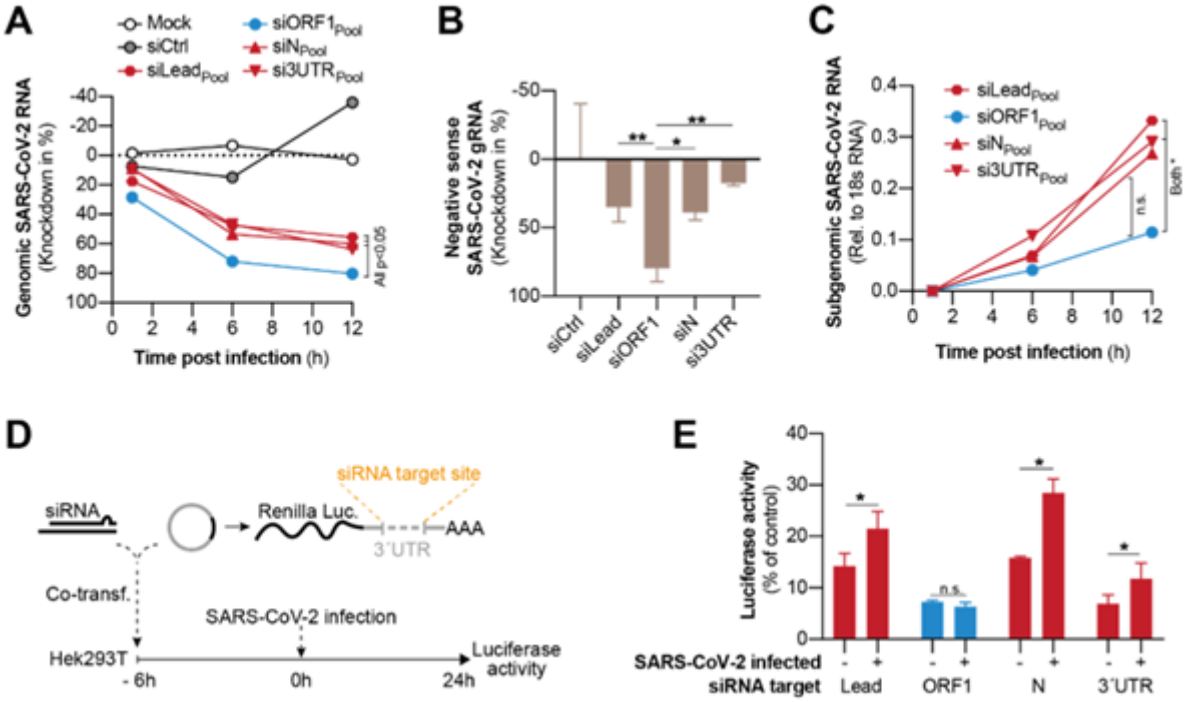

Figure 4

[Please see the manuscript file to view figure caption.]

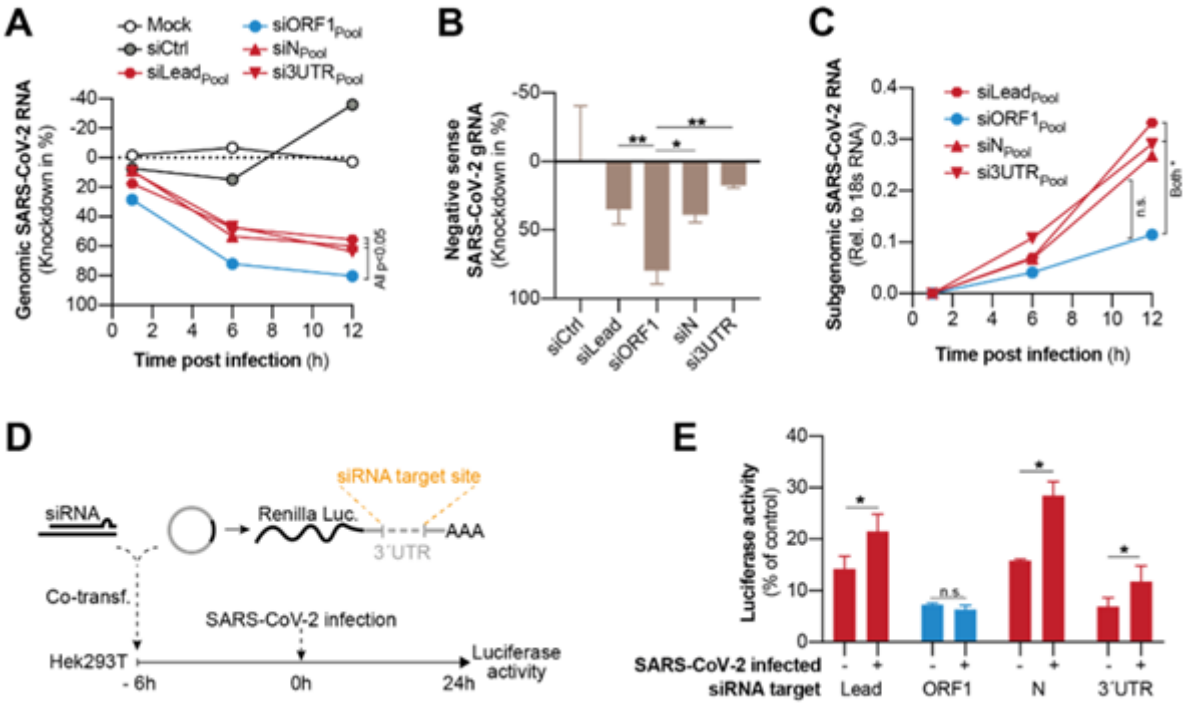

Figure 4

[Please see the manuscript file to view figure caption.]